Flexible a-IGZO phototransistor for instantaneous and cumulative UV-exposure monitoring for skin health

Article (Accepted Version)

DOI: 10.1002/((please add manuscript number))
Article type: Communication

Flexible a-IGZO phototransistor for instantaneous and cumulative UV-exposure monitoring for skin health

Stefan Knobelspies, Alwin Daus, Giuseppe Cantarella, Luisa Petti, Niko Münzenrieder, Gerhard Tröster and Giovanni Antonio Salvatore*

S. K. Author 1, A. D. Author 2, G. C. Author 3, L. P. Author 4, G. T. Author 6, G. A. S. Author 7
Electronics Laboratory, Swiss Federal Institute of Technology (ETH) Zürich, Gloriastrasse 35, 8092 Zürich, Switzerland
E-mail: stefan.knobelspies@ife.ee.ethz.ch
N. M. Author 5
Sensor Technology Research Center, School of Engineering and Informatics, University of Sussex, Falmer, Brighton BN1 9QT, United Kingdom

Keywords: ultraviolet light sensors (UV-sensors), amorphous Indium-Gallium-Zinc-Oxide (a-IGZO), flexible electronics, thin-film-transistors (TFTs)

Abstract

The accurate and continuous monitoring of both instantaneous and cumulative exposure to UV-light is of great relevance for dermatology and skin care to avoid damages to the dermis and epidermis and, ultimately, prevent melanoma. Here, we demonstrate flexible thin-film phototransistors based on amorphous Indium-Gallium-Zinc-Oxide (a-IGZO) semiconductor whose optical band-gap (3.05 eV) enables monitoring of the entire UV-spectrum. At the same time, the device structure together with a new read-out scheme consisting of a rectangular modulation of the gate-source voltage allow for both real time and cumulative measurement of UV-light intensity. Thanks to its design and thickness, the optoelectronic properties of the sensor remain unaffected after 2000 bending cycles down to radii of 6 mm. Furthermore, the device can be encapsulated with a thin Polydimethylsiloxane (PDMS) layer to achieve a compliant adhesion with the skin and enable wearable applications.

Ultraviolet (UV) radiation, which is part of the sunlight spectrum with wavelengths ranging from 280 nm to 400 nm, is considered as one of the main cause of melanoma skin cancers[1]. It is estimated that one out of five Americans will develop skin cancer in their lifetime[2]. As Earth's protective ozone layer becomes thinner[3] the prevention of exposure to dangerous UV-intensities is of crucial interest[4]. Data on instantaneous and cumulative UV exposures provide important information for dermatology, skin and general healthcare and eventually help to prevent damages to the dermis, epidermis[5] or eyes[6]. Wearable and, more recently, epidermal or skin-like devices, such as UV-dosimeter temporary tattoos[7] or highly stretchable photodetectors[8] have shown great potential to achieve accurate and unobtrusive sensing of important bio-signals and represent a promising technology for health monitoring[9,10].

Among the palette of materials, wide bandgap semiconductors, such as ZnO and its composites (Indium-Gallium-Zinc-Oxide (IGZO), Indium-Zinc-Oxide (IZO), Zinc-Tin-Oxide (ZTO), etc.) can be used for UV-photodetection[11]. Research in recent years has established amorphous IGZO (a-IGZO) as one of the most promising semiconductors for thin-film transistors[11] thanks to its attractive properties including high mobility (10 cm^2/Vs)[12], low temperature and large area deposition, operational stability[13] and the suitability for integration into flexible electronics[14]. Such technology could also replace polysilicon in the active matrix of displays[15] which could benefit from the integration of UV-light sensors for automated adaption of display brightness to the environmental illumination conditions. In addition, the optical bandgap of a-IGZO is ~3.05 eV[16], which makes this material an excellent candidate for detection of the whole UV-spectrum[17] in contrast to ZnSnO or ZnO which have bandgaps around 3.3 eV[18,19], corresponding to 368 nm (**Figure 1** (a)). The measured optical absorption of a 20 nm thick a-IGZO layer deposited by magnetron sputtering at room temperature is measured by UV-vis spectroscopy and presented in

Figure 1 (b). The curve shows that the absorption rises as soon as the light wavelength reaches the UV-regime. Furthermore, Figure 1 (b) presents the spectra of the LED light sources used for the light-dependent characterization of the fully fabricated sensors.

The photofield-effect and the photosensitive characteristics of rigid a-IGZO TFTs have been widely studied[16,20]. One main drawback of such devices, as well as of ZnSnO[21] TFTs, is the long recovery time (in the range of 12-22 hours)[20,21] which limits the sensor operations for real time detection. To date, there are only few reports on a-IGZO TFT based UV-sensors with a recovery time in the range of seconds[22] but they are based on rigid structures. Other approaches, using rigid ZnO TFT based UV-sensors, are unattractive for mobile devices because of their high operating voltage[19]. ZnO nanowires can also be employed as semiconductor material in thin film transistors for instantaneous UV-light measurements[23] but their higher sensitivity, thanks to the increased surface to volume ratio, usually comes at costs of more complex processing.

In this communication, we present a mechanically flexible a-IGZO thin-film transistor (TFT) based UV-sensor fabricated on free-standing polyimide foil (Kapton E), and then encapsulated in a thin and transparent Polydimethylsiloxane (PDMS) layer which enables direct lamination on skin. Furthermore, we show a new measurement concept based on a rectangular AC modulation of the gate-source voltage (V_{GS}) which simultaneously enables real-time detection and the read-out of the cumulative dosage due to the long-term charge carrier storage in the gate dielectric[24]. Our device enables a low operating voltage of 6 V and a low power consumption of about 1 mW. In addition to skincare, our approach is also compatible with state-of-the art process technology used for display applications, due to similar device architecture as well as compatible materials[11,25]. This prospects the application of a-IGZO TFTs for both pixel driving, as well as for UV-sensing and light intensity adaptation.

The a-IGZO TFTs are designed employing a bottom-gate configuration and fabricated at low temperature on free-standing polyimide foils to allow large area processing (see the experimental section for more details). Figure 1 (c) shows a sketch of the device and highlights the active layers and the substrate/encapsulation stack. The transfer characteristic of a TFT is shown in the **Figure S1.** The electrical characteristics yield a current on/off ratio in the order of 10^7, a linear mobility of 20.07 $cm^2 \cdot V^{-1} \cdot s^{-1}$ and a threshold voltage V_{Th} = 0.72 V, which are in line with state-of-the-art values for these devices[26]. Additionally, the device is encapsulated by thin PDMS layers, which offer an optical transparency down to wavelengths of 240 nm[27] hence including the entire UVA and UVB spectrum. Furthermore, PDMS provides a good adhesion to the human skin and high bendability/stretchability to adapt to the shape of a finger, as presented in the photographs of Figure 1 (d) and **Figure S2**. Despite the transistor structure comes at costs of a more complicated fabrication process compared to passive devices as photodiodes, it offers various advantages: (i) it possesses an internal amplification resulting in higher sensitivities; (ii) it provides the possibility to tune the operating range of the sensor by properly setting the biasing conditions; (iii) it combines sensing and multiplexing capabilities in one compact device structure which enables scalability for multi-pixel applications.

The time-dependent TFT drain current (I_D) serves as sensor signal in response to illumination (with V_{DS} = 3 V and V_{GS} = -3 V/+3 V). Initially, the cross sensitivity of the device for red, green, blue and UV-light is evaluated and the I_D is normalized over the corresponding light intensity (**Figure S3**). As expected from the IGZO band gap, the sensor shows a larger change in I_D for smaller wavelengths. Since red ($\lambda_{Peak,red}$ = 623 nm), blue ($\lambda_{Peak,blue}$ = 470 nm) and green ($\lambda_{Peak,green}$ = 525 nm) wavelengths are smaller than the band gap of a-IGZO ($\lambda_{bandgap,IGZO}$ = 406 nm), the sensor response at such wavelengths is attributed to light absorption at defects located either in the a-IGZO and/or at the Al_2O_3/IGZO interfaces[28]. Nevertheless, the change in I_D is 220, 3600 and 37600 times larger for the UV-light,

compared to blue, green and red light, respectively. Therefore, the interference through the visible light spectrum can be considered negligible. In agreement with previously reported works[20], the measured relaxation time of the drain current in darkness after exposure is about 8-12 hours. Such long retention offers valuable and enduring information about the exposure history but prevents the acquisition of information regarding the instantaneous light intensity.

Figure 2 (a) introduces and describes a new measurement technique that overcomes the abovementioned issues and provides information on both cumulative and instantaneous exposure to UV-light. The V_{GS}, is modulated with a rectangular-shaped signal. Without illumination, the drain current shows almost static plateaus which are responding in phase with the gate modulation. Under illumination, the drain current I_D contains two components:

$$I_D = I_{D,stat} + \Delta I_{D,trans} \quad (1)$$

(i) a static response $I_{D,stat}$ which is caused by the shift of the threshold voltage (see **Figure S4** for a representative shift of the transfer characteristic) and accounts for the illumination history; (ii) a transient response $\Delta I_{D,trans}$ which occurs when switching V_{GS} from negative to positive and whose peak height (at constant measurement frequency) is related to the actual UV-intensity and is independent of the illumination history. The accumulated UV-dosage value is stored in the baseline ($I_{D,stat}$) with a retention time of hours. Figure 2 (b) shows an extract of the measurement for two different UV-intensities. The transistor is biased with V_{DS} = 3 V and additionally a rectangular AC modulation of V_{GS} (-6 V/+6 V) at 100 mHz and zero DC component is applied. A complete measurement example can be found in **Figure S5**. Figure 2 (c) shows a magnified view of the measurement and highlights the two components of the raw signal: transient response exclusively due to the instantaneous illumination (top of the figure) and a fit of the static response which is the result of the illumination history (bottom of the figure). The dependence of the peak height on the light-intensity is estimated by repeating the experiment with intensities ranging from 0.2 to 2.4 $mW \cdot cm^{-2}$. Figure 2 (d) presents the resulting linear dependence. The sensitivity S is defined as

$$S = \delta\Delta I_{D,trans} / \delta\text{UV-intensity} \quad (2)$$

, resulting in a value of 4.14 µA/(mW·cm^{-2}).

For flexible applications, the device stability under bending is of prior interest. Devices with similar structure, material composition and substrate thicknesses have shown the ability to bend down to few mm radii without any significant degradation of the electrical performance[29,30]. Consequently, the long-term mechanical stability is analyzed by repeatedly bending-flattening the device to a tensile radius of 6 mm for 2000 cycles (corresponding strain ε = 0.37 %) using an automated bending setup (see **Figure S6** (a) in SI)[30]. The response to 2 mW·cm^{-2} UV-intensity is characterized under same TFT biasing conditions before and after the cyclic bending and the results are compared in Figure S6 (b) and (c). The drain current response remains unchanged in height and shape after the bending tests. A possible delamination of the Polyimide foil from the PDMS encapsulation is investigated by stretching experiments, which demonstrates the structural stability of the sensor system even under strain up to 25.8 % as shown in **Figure S7**. One should note, that just the PDMS is stretched while the Polyimide remains as stiff island, which can be referred to approaches on soft/hard integration in stretchable electronics[31].

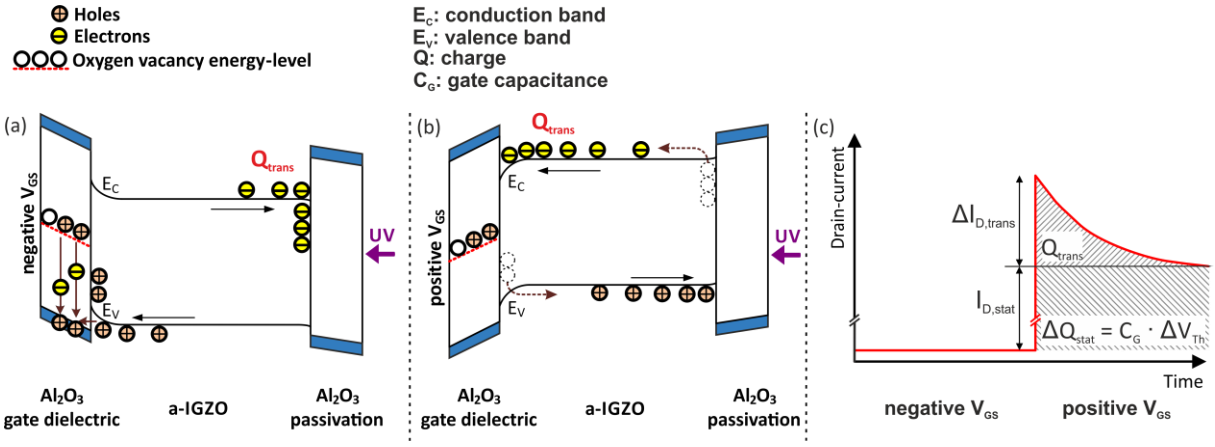

Figure 3 displays a schematic explanation about the physical origin of the transient, as well as the static UV-response of the sensor. According to previous work[16], when IGZO is illuminated by UV-light, electron-hole pairs are generated in the semiconductor. By applying

a negative V_{GS}, the conduction- and valence band of the IGZO are bent upwards as illustrated in Figure 3 (a). In this case, the generated electrons inside the IGZO are pushed away from the gate dielectric due to the repulsing force of the electric field between gate and source and are accumulated and trapped at the top IGZO/Al_2O_3 passivation interface. The generated holes are attracted towards the gate dielectric interface. They are able to get injected into the valence band of the gate insulator[24] due to small valence band offsets between Al_2O_3 and IZGO, as well as getting trapped at the IGZO/Al_2O_3 interface[32]. Inside the Al_2O_3 they recombine with the electrons from oxygen vacancies in the dielectric, resulting in positive charges inside these vacancy levels. These charges lead to a persistent and negative shift of V_{Th} and therefore to an increased $I_{D,stat}$[24]. When switching the V_{GS} to a positive value, as shown in Figure 3 (b), the electrons inside the conduction band of IGZO can drift into the channel area and the trapped electrons at the IGZO/Al_2O_3 passivation interface are released due to the high electric field, where they contribute to the drain current. Such electrons are responsible of the transient peaks of the drain current $\Delta I_{D,trans}$. The shape of the transient $\Delta I_{D,trans}$ peaks is in agreement with previously reported stretched exponential modeling of the de-trapping process[33,34]. Though the positive charges inside the Al_2O_3 gate insulator and therefore the V_{Th} shift occur to be unaffected by the alternating V_{GS}. Figure 3 (c) qualitatively illustrates the change in I_D as result of the charge generation-recombination and transport in the Al_2O_3 and a-IGZO layer for positive and negative biasing and for constant light intensity. It is worth mentioning that for reliable operation and for practical use cases, the device should always be powered. Nevertheless, in the scenario of non-continuous measurements, the first $\Delta I_{D,trans}$ peak should be disregarded and the second peak considered.

It can be concluded that the instantaneous response is due to the alternating gate biasing which switches the device between the on and off states. As a verification different modulation for V_{GS} were tested. **Figure S8** in the SI shows the result for a V_{GS} having an offset of 4 V and an AC component of ±1 V. In this configuration, the transistor is never

switched off, thus no temporary electron storage occurs and no peak in the drain current is observed in agreement with the above described physical mechanism.

In summary, we presented a mechanically flexible thin-film phototransistor based on a-IGZO semiconductor whose bandgap of 3.05 eV enables the absorption of wavelengths < 406 nm, which cover the entire UV-spectrum and are thus relevant for skincare applications. The device architecture and a new measurement technique consisting of a rectangular modulation of the gate-source voltage lead to a transient signal response, giving information about the real-time UV-intensity. Simultaneously, positive charge trapping occurring in the Al_2O_3 gate dielectric allows for cumulative UV-dosage measurements. The devices are fabricated on a thin Polyimide foil and encapsulated with transparent PDMS thin films to ensure unaltered optoelectronic functionalities even after 2000 bending cycles to a radius of 6 mm and enable compliant lamination with skin. Additionally to skin care, it would be even possible to fabricate these devices entirely transparent[35], opening the way to the integration into bendable edge-to-edge displays or contact lenses.

Experimental Section

Fabrication: The flexible a-IGZO TFTs are fabricated in a bottom-gate inverted staggered configuration on a 50 µm thick flexible polyimide foil, as shown schematically in Figure 1 (c)[29]. Contaminations and residuals are removed by cleaning the substrates with acetone and isopropanol (in an ultrasonic bath), followed by a subsequent heating at 200°C for 24 hours. A 50 nm SiN_x buffer layer is deposited on both sides of the substrate by plasma enhanced chemical vapor deposition (PECVD) to improve the adhesion of the subsequently deposited materials. The gate contact is formed by 35 nm thick electron-beam evaporated Cr which is structured by wet etching. Afterwards, a 25 nm Al_2O_3 gate dielectric is grown by atomic layer deposition (ALD) at 150 °C. Next, room temperature RF magnetron sputtering of 20 nm a-IGZO combined with wet etching are used to form the active channel area. After

structuring the contact vias into Al_2O_3 by wet etching, an electron beam evaporated Ti/Au (10/60 nm) layer serves as source and drain electrodes. Finally, the TFTs are passivated by a second ALD-deposited 25 nm thick Al_2O_3 film. For wearable, on-skin or skin-like applications, the TFTs are transferred on a 50 µm thick spin-coated PDMS layer, wired and further encapsulated with a second PDMS layer (50 µm thick), to achieve adhesion on human skin as illustrated in Figure 1 (d).

Characterization: The electrical characterization (see Figure S1) is performed with a semiconductor device analyzer (Agilent technologies, B1500A). The TFT yields a current on/off ratio in the order of 10^7, a mobility of 20.07 $cm^2 \cdot V^{-1} \cdot s^{-1}$, a threshold voltage of V_{Th} = 0.72 V and a W/L ratio of 280/80. The time dependent TFT drain current (I_D) response to illumination is characterized at room temperature and the illumination intensity and wavelength is varied throughout the experiments. For the light-dependent measurements, sensors without PDMS encapsulation are used. A custom-made measurement setup is utilized, which allows for mounting the respective LED light-sources (UV: Optosource, 260019 SERIES, peak wavelength 375 nm[36]; RGB: TTElectronics/Optek Technology OVLBx4C7 Series[37]) in a defined distance of 25 mm to the sensor, while electrically connecting the devices with probe needles. The complete setup is placed in a dark box to avoid interferences by ambient light. The LED-current is controlled via LabVIEW and a HP E3631 power supply while the TFT output signals are measured with the semiconductor device analyzer.

Bending and stretching experiments: The cyclic bending is performed without incident illumination with the setup presented in Figure S6. Here, a sample without PDMS encapsulation is used, which is mechanically fixed on one side and clamped into a movable support on the other side. The translatory movement of the movable part is controlled via a step motor. Two thousand bending-flattening cycles are performed and the sensing characteristics before and after are compared. Possible delamination of the device fabricated on Polyimide foil from thin and soft PDMS encapsulation layers is optically analyzed while

applying strain up to ε = 25.8 %. Experimental results demonstrate that no delamination occurs (Figure S7).

Mounting on skin: The device in laminated on the skin with the help of a 25 µm thick double side medical tape (Acrylic adhesive, Scapa Healthcare). The device can be removed after use and re-used multiple times.

Supporting Information

Supporting information is available from the Wiley Online Library or from the author.

Acknowledgement

This work is supported by a grant from the Schweizer Nationalfond (SNF), Switzerland through the project "WISDOM: Wireless Indium-Gallium-Zinc-Oxide Transmitters and Devices on Mechanically-Flexible Thin-Film Substrates". The authors wish to thank Weyde Lin for his support in the optical measurements.

Received: ((will be filled in by the editorial staff))
Revised: ((will be filled in by the editorial staff))
Published online: ((will be filled in by the editorial staff))

[1] B. K. Armstrong, A. Kricker, *J. Photochem. Photobiol. B Biol.* **2001**, *63*, 8.

[2] J. K. Robinson, *JAMA* **2005**, *294*, 1541.

[3] F. Anwar, F. N. Chaudhry, S. Nazeer, N. Zaman, S. Azam, *Atmos. Clim. Sci.* **2016**, *6*, 129.

[4] X. Zhang, W. Xu, M.-C. Huang, N. Amini, F. Ren, in *Proc. 8th Int. Conf. Body Area Networks*, ACM, **2013**.

[5] M. Ichihashi, M. Ueda, A. Budiyanto, T. Bito, M. Oka, M. Fukunaga, K. Tsuru, T. Horikawa, *Toxicology* **2003**, *189*, 21.

[6] F. J. G. M. Van Kuijk, *Environ. Health Perspect.* **1991**, *96*, 177.

[7] L'Oréal, "L'Oréal debuts first-ever stretchable electronic UV monitor at the 2016 consumer electronics show," can be found under http://www.loreal.com/media/press-releases/2016/jan/loreal-debuts-first-ever-stretchable-electronic-uv-monitor, **2016**.

[8] C.-W. Chiang, H. Golam, W.-C. Tan, Y.-R. Liou, Y.-C. Lai, R. Ravindranath, H.-T. Chang, Y.-F. Chen, *ACS Appl. Mater. Interfaces* **2015**, acsami.5b09373.

[9] D.-H. Kim, N. Lu, R. Ma, Y.-S. Kim, R.-H. Kim, S. Wang, J. Wu, S. M. Won, H. Tao, A. Islam, K. J. Yu, T. Kim, R. Chowdhury, M. Ying, L. Xu, M. Li, H.-J. Chung, H. Keum, M. McCormick, P. Liu, Y.-W. Zhang, F. G. Omenetto, Y. Huang, T. Coleman, J. A. Rogers, *Science (80).* **2011**, *333*, 838.

[10] X. Huang, Y. Liu, K. Chen, W. J. Shin, C. J. Lu, G. W. Kong, D. Patnaik, S. H. Lee, J. F. Cortes, J. A. Rogers, *Small* **2014**, *10*, 3083.

[11] X. Yu, T. J. Marks, A. Facchetti, *Nat. Mater.* **2016**, *15*, 383.

[12] K. Nomura, H. Ohta, A. Takagi, T. Kamiya, M. Hirano, H. Hosono, *Nature* **2004**, *432*, 488.

[13] R. F. Service, *Science (80-.).* **1997**, *278*, 383.

[14] L. Petti, N. Munzenrieder, C. Vogt, H. Faber, L. Buthe, G. Cantarella, F. Bottacchi, T. D. Anthopoulos, G. Troster, *Appl. Phys. Rev.* **2016**, *021303*, 1.

[15] I.-J. Chung, I. Kang, *Mol. Cryst. Liq. Cryst.* **2009**, *507*, 1.

[16] T. Fung, C. Chuang, K. Nomura, H. D. Shieh, H. Hosono, J. Kanicki, *J. Inf. Disp.* **2008**, *9*, 21.

[17] J. L. Lean, G. J. Rottman, H. L. Kyle, T. N. Woods, J. R. Hickey, L. C. Puga, *J. Geophys. Res.* **1997**, *102*, 29939.

[18] H. Y. Jung, Y. Kang, A. Y. Hwang, C. K. Lee, S. Han, D.-H. Kim, J.-U. Bae, W.-S. Shin, J. K. Jeong, *Sci. Rep.* **2014**, *4*, 3765.

[19] H. S. Bae, S. Im, *Thin Solid Films* **2004**, *469-470*, 75.

[20] J. Yao, N. Xu, S. Deng, J. Chen, J. She, H. P. D. Shieh, P. T. Liu, Y. P. Huang, *IEEE Trans. Electron Devices* **2011**, *58*, 1121.

[21] P. Görrn, M. Lehnhardt, T. Riedl, W. Kowalsky, *Appl. Phys. Lett.* **2007**, *91*, 193504.

[22] W. Chen, H. Zan, *IEEE Electron Device Lett.* **2012**, *33*, 77.

[23] H. Kind, H. Yan, B. Messer, M. Law, P. Yang, *Adv. Mater.* **2002**, *14*, 158.

[24] B. Ryu, H.-K. Noh, E.-A. Choi, K. J. Chang, *Appl. Phys. Lett.* **2010**, DOI 10.1063/1.3464964.

[25] C.-T. Lee, Y.-Y. Huang, C.-C. Tsai, S.-F. Liu, C.-C. Kuo, C.-H. Chiu, C.-H. Huang, E.-C. Liu, S.-C. Huang, C.-L. Chen, C.-T. Liang, J.-S. Huang, *SID Symp. Dig. Tech. Pap.* **2015**, *46*, 872.

[26] G. Cantarella, N. Münzenrieder, L. Petti, C. Vogt, L. Büthe, G. A. Salvatore, A. Daus, G. Tröster, *IEEE Electron Device Lett.* **2015**, *36*, 781.

[27] M.-H. Wu, K. E. Paul, G. M. Whitesides, *Appl. Opt.* **2002**, *41*, 2575.

[28] H.-K. Noh, K. J. Chang, B. Ryu, W.-J. Lee, *Phys. Rev. B* **2011**, *84*, 115205.

[29] N. Münzenrieder, C. Zysset, T. Kinkeldei, G. Tröster, *Semicond. Conf. Dresden (SCD), 2011* **2011**, 1.

[30] N. Munzenrieder, K. H. Cherenack, G. Troster, *IEEE Trans. Electron Devices* **2011**, *58*, 2041.

[31] S. Wagner, S. Bauer, *MRS Bull.* **2012**, *37*, 207.

[32] K. Nomura, T. Kamiya, H. Hosono, *Appl. Phys. Lett.* **2011**, *99*, 129.

[33] J. M. Lee, I. T. Cho, J. H. Lee, H. I. Kwon, *Appl. Phys. Lett.* **2008**, *93*, 11.

[34] T. C. Chen, T. C. Chang, C. T. Tsai, T. Y. Hsieh, S. C. Chen, C. S. Lin, M. C. Hung, C. H. Tu, J. J. Chang, P. L. Chen, *Appl. Phys. Lett.* **2010**, *97*, DOI 10.1063/1.3481676.

[35] G. a Salvatore, N. Münzenrieder, T. Kinkeldei, L. Petti, C. Zysset, I. Strebel, L. Büthe, G. Tröster, *Nat. Commun.* **2014**, *5*, 2982.

[36] Optosource, "Datasheet - Reference 30/99 Issue 02," can be found under http://datasheet.octopart.com/260019-Marl-datasheet-8611908.pdf, **n.d.**

[37] TTElectronics/Optec Technology, "Datasheet - Issue A.1 (06/07)," can be found under http://optekinc.com/datasheets/OVLBB4C7.pdf, **n.d.**

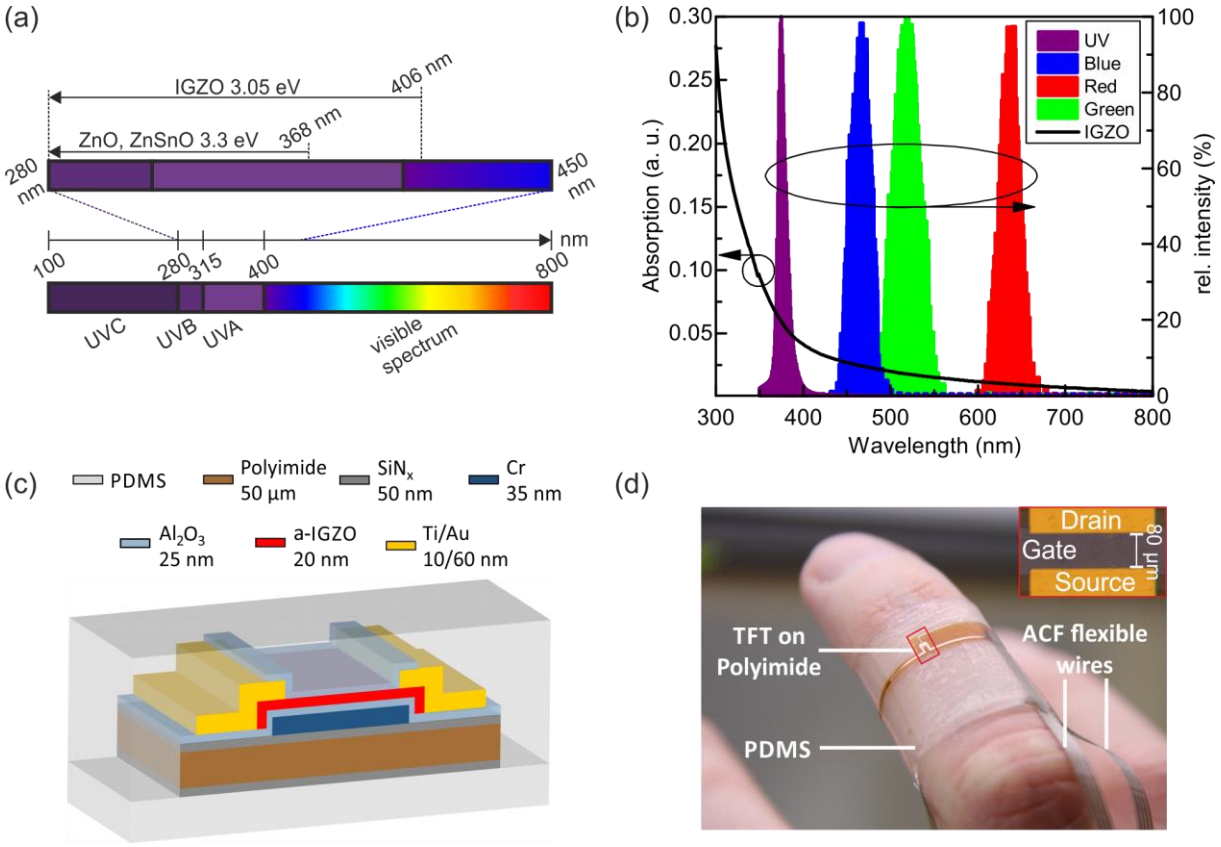

Figure 1. ***(a)*** *UV- and visible light spectra and the respective absorption areas of IGZO*[16]*, ZnSnO*[18] *and ZnO*[19]*.* ***(b)*** *The spectra of the red, green, blue and UV LED light sources as well as the optical absorption of the a-IGZO layer.* ***(c)*** *Schematic device cross-section with layer stack and thicknesses of a TFT and the proposed PDMS encapsulation.* ***(d)*** *A real-life application example of the TFT-based sensor. By encapsulating the sensor into PDMS, it can placed on human skin and the wires can directly be connected to a readout device.*

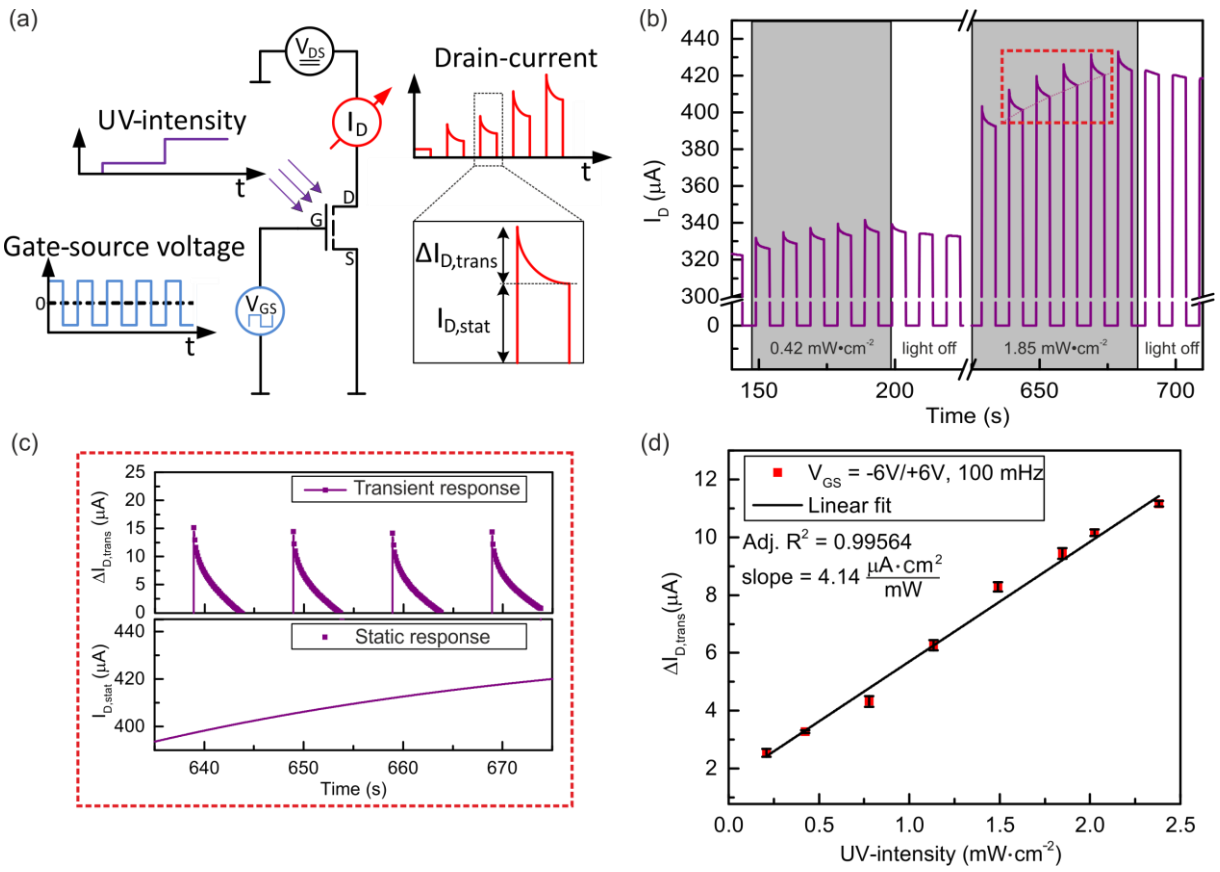

Figure 2. (a) *Schematic circuit diagram of the measurement protocol. V_{GS} is modulated with a rectangular AC signal (without DC-offset) and V_{DS} is kept constant. I_D is measured and the resulting drain current peak heights $\Delta I_{D,trans}$ correspond to the incident UV-intensity. The static change in drain current $I_{D,stat}$ represents the memory effect of UV-dosage seen by the sensor.* ***(b)*** *Visualization of the a-IGZO TFT based UV-sensor response that is used for the real-time measurement. Two different UV-intensities (0.42 mW·cm^{-2}and 1.85 mW·cm^{-2}) are shown here. The TFT is biased with V_{DS} = 3 V and a V_{GS} (rectangular shaped, V_{GS} = ±6 V). Under illumination, the peak height of the temporary offset current $\Delta I_{D,trans}$ is directly related to the UV-intensity and independent of the static I_D-offset $I_{D,stat}$.* ***(c)*** *The magnified area highlights the two components of the sensor signal: the transient response $\Delta I_{D,trans}$ and the fitted static response $I_{D,stat}$.* ***(d)*** *Relation between the transient peak height of $I_{D,trans}$ and UV-intensity at a V_{GS} modulation frequency of 100 mHz. A linear fit is added which shows a sensitivity of $\delta\Delta I_{D,trans}/\delta$UV-intensity = 4.14 μA/(mW·cm^{-2}).*

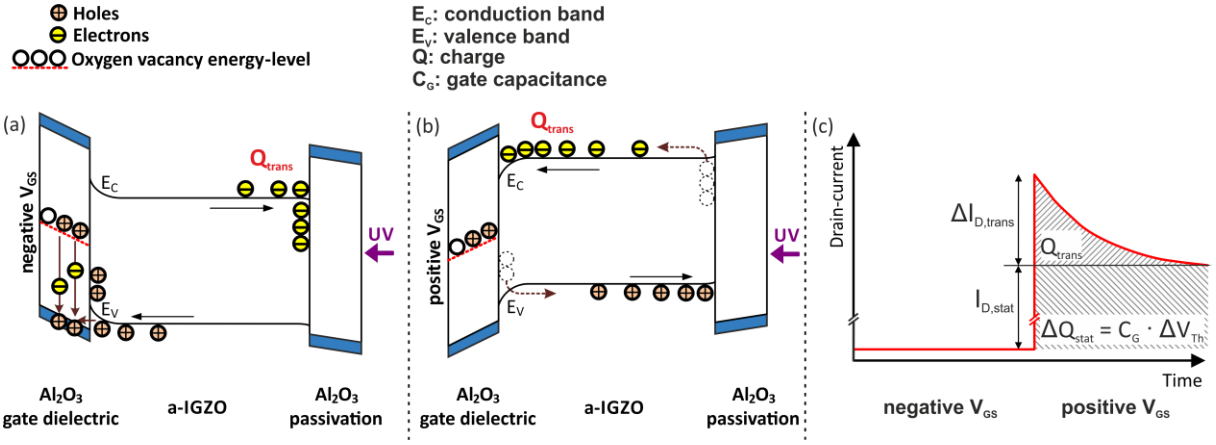

Figure 3. *Schematic of the photo- and interface effects in the IGZO and Al_2O_3 layers, as well as in the interfaces (respective layer stack for both cases: (left) gate insulator, (middle) a-IGZO semiconductor, (right) top passivation) under UV-illumination for two different cases:* ***(a)*** *negative and* ***(b)*** *positive V_{GS}.* ***(c)*** *The resulting change in drain current (static $I_{D,stat}$ and transient $\Delta I_{D,trans}$) due to the alternating V_{GS} and UV-illumination is schematically shown.*

Flexible thin-film phototransistors based on amorphous Indium-Gallium-Zinc-Oxide (a-IGZO) semiconductor and a novel read-out scheme allows for both real time and cumulative measurement of the ultraviolet (UV) light intensity. Furthermore, encapsulation in PDMS and lamination to human skin, as well as mechanical stability of the device is presented.

Keywords: ultraviolet light sensors (UV-sensors), amorphous Indium-Gallium-Zinc-Oxide (a-IGZO), flexible electronics, thin-film-transistors (TFTs)

S. K.* Author 1, A. D. Author 2, G. C. Author 3, L. P. Author 4, N. M. Author 5, G. T. Author 6, G. A. S. Author 7

Flexible a-IGZO phototransistor for instantaneous and cumulative UV-exposure monitoring for skin health

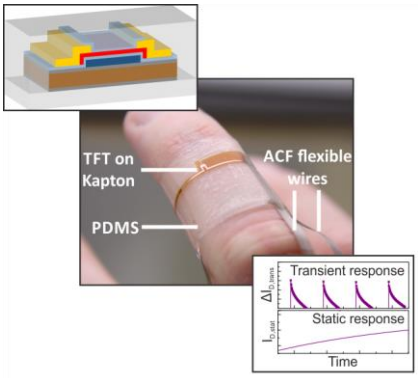

Supporting Information

Flexible a-IGZO phototransistor for instantaneous and cumulative UV-exposure monitoring for skin health

Stefan Knobelspies, Alwin Daus, Giuseppe Cantarella, Luisa Petti, Niko Münzenrieder, Gerhard Tröster and Giovanni Antonio Salvatore*

Transfer characteristic of the thin-film transistor (TFT)

The transfer characteristic of the a-IGZO TFT (with a drain-source voltage of V_{DS} = 3 V) is measured with a semiconductor device analyzer (Agilent technologies, B1500A) and shown in figure S1. The TFT yields a current on/off ratio in the order of 10^7 and a threshold voltage V_{Th} = 0.72 V and a linear mobility of μ_{lin} = 20.07 $cm^2 \cdot V^{-1} \cdot s^{-1}$.

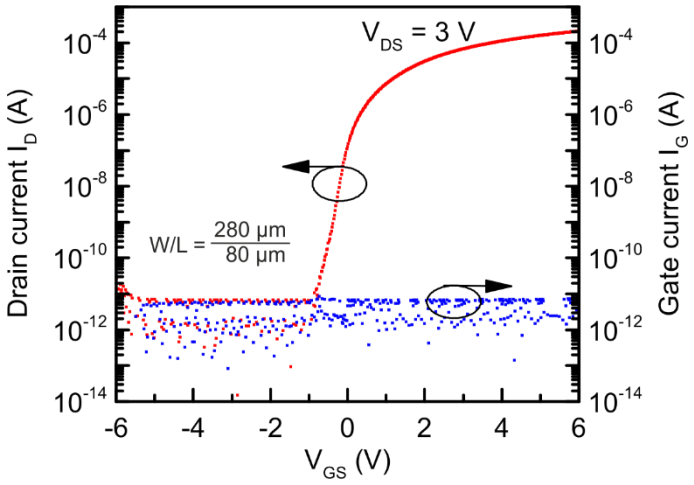

Figure S1. *The transfer characteristic of the a-IGZO TFT (with a drain-source voltage of V_{DS} = 3 V).*

Placement on skin

The TFTs which are encapsulated between two PDMS layers, which offer a good adhesion to human skin. Also, this layer offers removal and multiple time re-usage of the sensors. Application examples are shown in Figure S2.

Figure S2. Examples for the device placement: (a) on the upper arm; (b) wrinkled on the upper arm; (c) on the wrist.

Light dependent measurements

The time dependent TFT drain current response to illumination (with V_{DS} and V_{GS} at fixed values) is characterized at room temperature and the illumination intensity and wavelength is varied throughout the experiments. The measurements are performed in darkness to avoid interferences by ambient light. The UV-LED (peak wavelength 375 nm)[36] is mounted in a distance of 25 mm from the TFT and the LED-current is controlled with LabVIEW and a HP E3631 power supply. The response to UV-light and the cross sensitivity to visible light is analyzed with three additional LEDs of different wavelengths (red, green, blue).

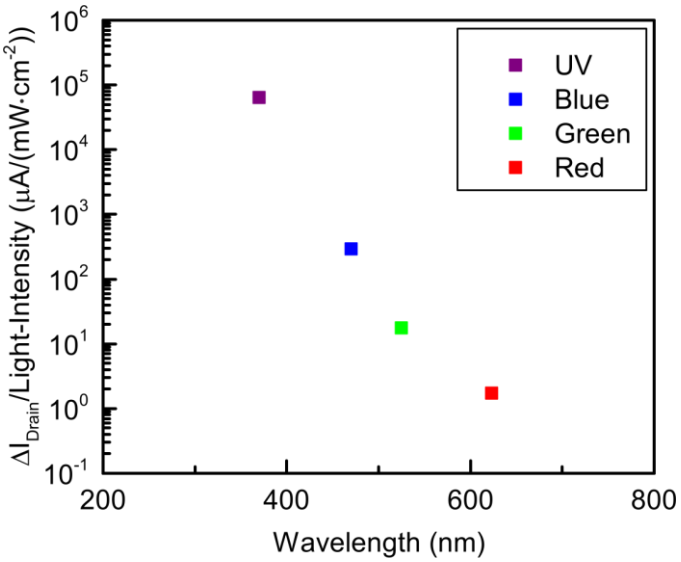

Figure S3. *The response of the drain current to red, green, blue and UV-light normalized to the respective light intensity, which shows a significantly higher response when the light energy is larger than the a-IGZO band gap.*

The UV-light induced shift of the transfer characteristic is presented in Figure S4. With increasing UV-intensity, a negative shift occurs.

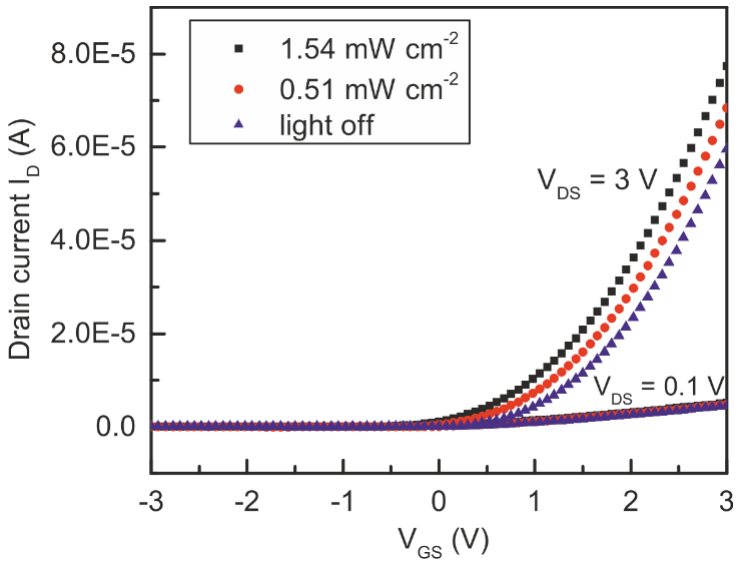

Figure S4. *Shift of the TFT transfer characteristic in dependence of the incident UV-intensity.*

The raw signal of a measurement of UV-intensities in the range of 0.2 mW·cm^{-2} to 2.4 mW·cm^{-2} is shown in figure S5. The measurement is performed with the new proposed measurement technique at V_{DS} = 3V and rectangular modulated V_{GS} = -6 V/+6 V (at 100 mHz).

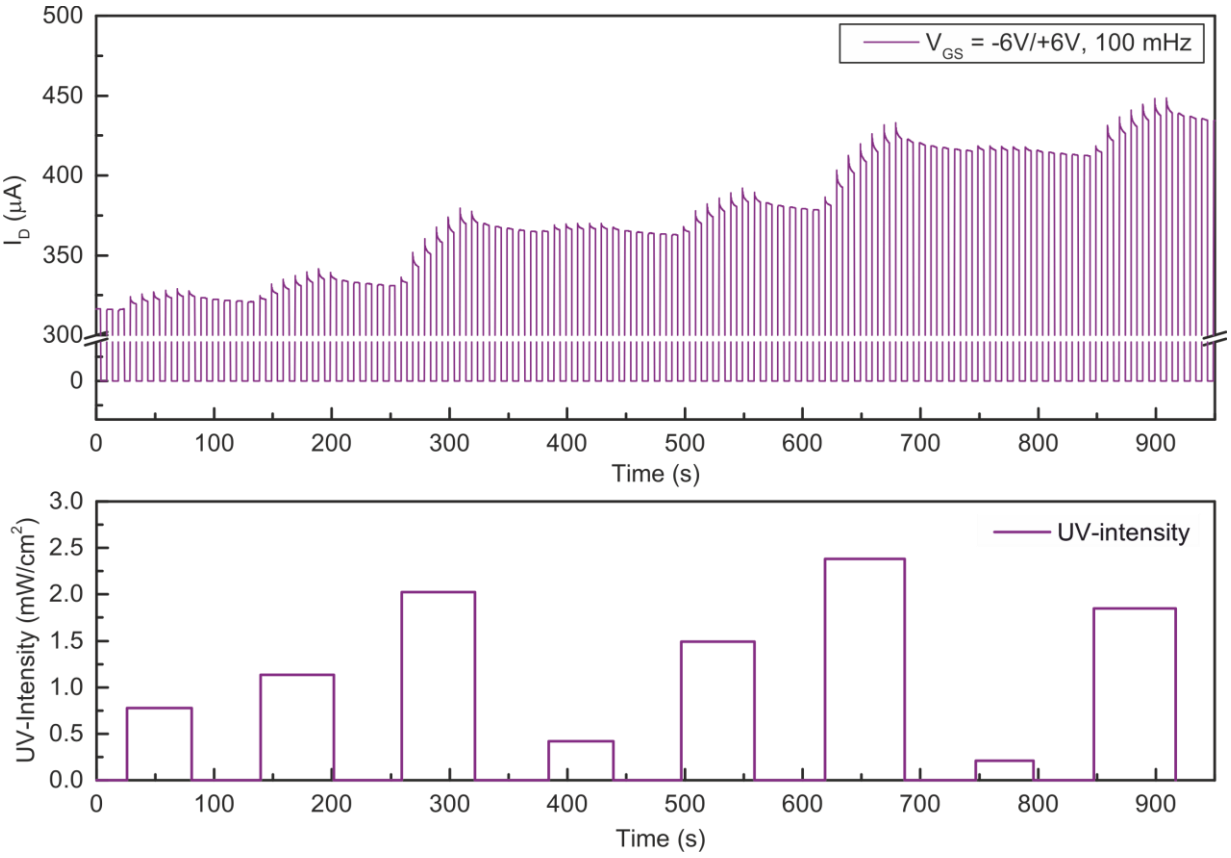

Figure S5. *Complete measurement of the a-IGZO TFT UV-sensor at varying UV-intensities using the novel measurement technique. The UV-intensities are applied in random order to proof the offset independence of the extracted sensor signal. Furthermore, it is visible, that the increase in $I_{D,stat}$ is a cumulative effect depending on the applied UV-intensity.*

Bending and stretching Experiments

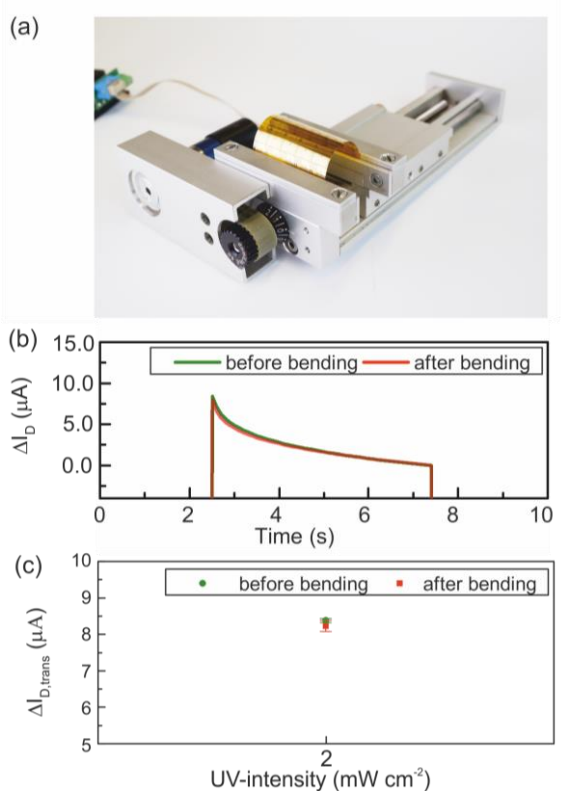

Figure S6. *(a) Setup for automatized cyclic bending of the devices. (b) A single transient peak from a measurement of the a-IGZO TFT based UV-sensor exposed with 2 mW·cm^{-2} UV-intensity before and after 2000 bending cycles down to a tensile radius of 6 mm. The peaks are normalized to their corresponding baselines. (c) Averaged evaluation of the $\Delta I_{D,trans}$ peak-heights (at 2 mW·cm^{-2} UV-intensity) before and after bending. The slight offset shift is most probably attributed to a small change in the LED-to-sensor alignment due to mounting and unmounting the devices for the cyclic bending.*

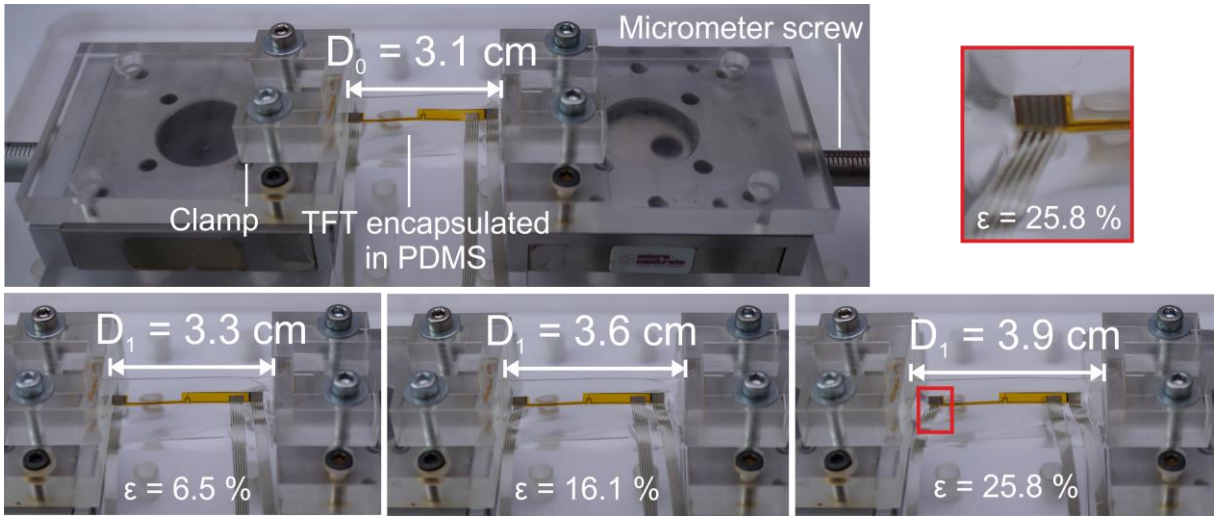

Figure S7. *Stretching experiment for the device encapsulated in PDMS. The PDMS layer is clamped into two adjustable supports, which can be moved accurately by micrometer screws. To analyze possible delaminating of Polyimide from PDMS, the devices are stretched to* $\varepsilon = 25.8\ \%$*. By optical observation, no delamination or breakage occurred.*

Further measurements

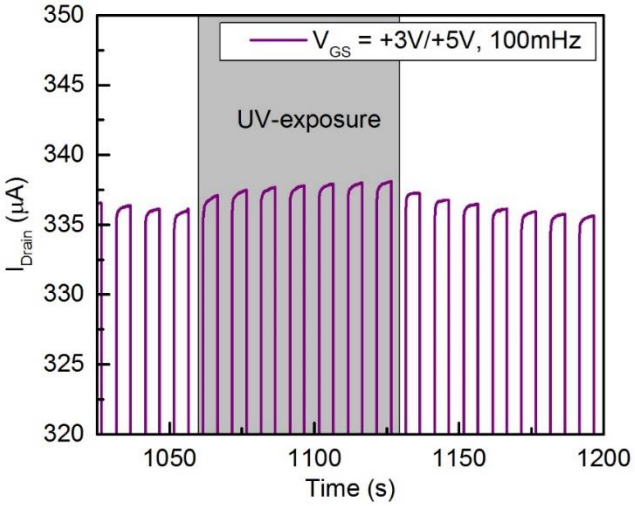

Figure S8. *The response of the TFT to 1.54 mW·cm^{-2} UV-illumination biased with a rectangular modulated V_{GS} at 100 mHz with an DC offset of 4 V and a peak-to-peak voltage of 2 V. With this configuration no transient current peaks occur as V_{GS} is always above V_{Th}.*